DOI: 10.6084/m9.figshare.16969876

LCC - № R895-920

A MATHEMATICAL MODEL OF TRANSPORT KINETICS OF 99MTC RADIOTRACERS

Oksana N. SHEVTSOVA [1]

[1] Department of Physical and Mathematical Sciences, the Faculty of Natural Sciences, National University of Kyiv-Mohyla Academy

Corresponding author: Oksana Shevtsova, Dr., o.shevtsova@ukma.edu.ua

Abstract. The proposed four-compartment mathematical model describes transport kinetics of 99m-technetium radiotracers at intravenous administration process with taking into account radiopharmaceutical accumulation, elimination and radioactive decay. The analytical solution of the model in a form of the well-known sum-of exponential solution was obtained. The dependencies of the tracer concentration versus the time are analyzed. The model can be easily verified by the radioactive tracer concentration data in the circulatory/lymphatic system measured at some time points, and the obtained data can be used to determine the transport coefficients. Time-activity dependencies were obtained and analyzed for each compartment. The model can be used for individual transport parameter calculation at administration of diagnostic/therapeutic dose loads.

Анотація. Запропонована 4-х компартментна математична модель описує транспортну кінетику 99m-технецієвих радіоактивних індикаторів при внутрішньовенному введенні препарату, враховуючи накопичення, елімінацію, радіоактивний розпад. Отриманий аналітичний розв’язок задачі у формі суми експоненціальних розв’язків. Проаналізовані залежності концентрації радіоактивного індикатора як функції часу. Модель може бути верифікована шляхом вимірювання концентрації радіоактивного індикатора у кровоносній/лімфатичній системі в певні моменти часу, а отримана інформація може бути використана для визначення транспортних коефіцієнтів. Залежність концентрації радіоактивного індикатора від часу отримана та проаналізована для кожного з компартментів.

Date of Review: 05.10.2021 7:10

ISSN 2311-1100

Модель можна застосовувати для обрахунку індивідуальних транспортних параметрів пацієнта при призначенні діагностичного/тератевтичного дозового навантаження

Keywords: Radiotracers, circulatory system, lymphatic system, transport kinetics of radiotracers, mathematical model.

Section: Physiological Systems Modeling

Introduction. The term “radiopharmaceutical” denotes the association of a radionuclide and pharmaceutical, i.e. symbiosis of biological, chemical and physical properties. Radiopharmaceuticals are approved for use in humans for diagnostic purposes chemical compounds whose molecules contain radionuclides. The method of diagnostics or radionuclide study of morphological and functional condition of the body using radionuclides or radionuclide-labeled indicators is one of the most common methods of detecting cancer. Radiopharmaceuticals are injected into the patient's body, and then using the radionuclide diagnostic devices it is possible to study the nature of their localization, retention, and removing them from the organs and tissues. Radiopharmaceuticals are selected with consideration of its radiopharmaceutical dynamic and nuclear-physical properties. Dynamics of radiopharmaceuticals is defined by a chemical compound that is the basis for radiopharmaceutical preparation. Registration of radiopharmaceutical is determined by the type of decay of the nuclide, by which it is marked. Some radiopharmaceuticals are called “radiotracers” because they are used only to diagnose (“trace”) dysfunctions in body tissues [1, 2, 3, 4].

A radiopharmaceutical introduced into the body is firstly uniformly distributed in the blood [5], and then selectively trapped by certain organs and tissues. Radiopharmaceuticals which are selectively accumulated in tumor tissues are called the tumor-imaging agents. They are mainly included in cells with a high mitotic and metabolic activity. Due to high concentration of radiopharmaceuticals a tumor area will emerge on a scintigram – the graphic record obtained by scintigraphy – as a hot site. This research technique is called positive scintigraphy. Areas with increased accumulation of a radiotracer are called hot areas; usually they correspond to overactive functioning body areas - areas of hyperplasia, some types of tumors, inflammatory tissue changes [6-10]. Radiopharmaceutical choice is caused by its pharmaceutical peculiarities and depends on tumor localization [6].

Radiopharmaceuticals are used in nuclear medicine as tracers for diagnostics and therapy of many diseases. Technetium 99m (^{99m}Tc) serves as gamma-rays-emitting tracer nuclide for many

radiopharmaceuticals. More than 30 different ^{99m}Tc based radiopharmaceuticals are known, which are used for imaging and functional studies in various organs, e.g. brain, lung, kidneys, liver, skeleton, etc. [7]. They also serve for diagnostic visualization of tumors. Their localization in the body is also determined by gamma-ray measurement.

Radiotracer dynamics are caused by different ways of radiotracer administration (intravenous, intradermal/subcutaneous, intratumoral, intraperitoneal). In the considered case of intravenous administration radiotracers are captured by the blood vessel, next depending on the size they move to the interstitium [14] and into the lymphatic system and are trapped by a sentinel lymph node of the lymphatic system.

The circulatory and the lymphatic system are the two vascular systems of the body. Besides the well-known major role of the lymphatic system in tissue fluid regulation, they are also important in tumor metastasis and immune system function. The circulatory system is made up of blood vessels that carry blood towards and from the heart. Arteries carry blood away from the heart and veins carry blood to the heart. The lymphatic system is a component of both the circulatory and the immune systems. The lymphatic system consists of a series of conduits (the lymphatic vasculature), lymphoid cells, and organized lymphoid tissues. Lymphoid tissues include the lymph nodes, spleen, thymus, Peyer's patches in the intestine, and lymphoid tissue in the liver, lungs, and parts of the bone marrow [12]. Lymphatic vessels are found throughout the body, with the exception of the central nervous system, where cerebrospinal fluid fulfills the normal role of lymph. Lymphatic vasculature and lymphoid tissue are prevalent in the organs that come into direct contact with the external environment, such as the skin, the gastrointestinal tract, and the lungs. This distribution is probably a reflection of the protective role of the lymphatic system against infectious agents and alien particles. Lymph, like venous blood, is under relatively low hydrostatic pressure. Flow through the lymphatic vessels cannot occur without the intervention of outside forces. These external forces include contraction of skeletal muscles, pressure changes owing to the action of breathing muscles and, for large lymphatic trunks, contraction of the wall's smooth muscles. Movement of the lymph in the vessels is unidirectional because the presence of valves prevents backflow [13]. Lymphatic system is the network of vessels through which lymph drains from the tissues into the blood.

Microcirculation plays a crucial role in the supply of oxygen and nutrients from the blood to extravascular tissues. The microcirculation system consists of blood and lymphatic vascular capillaries and the interstitium, and functional disorders of the microcirculation system are strongly related to, for example, inflammatory responses, swelling, and tumor [11].

The interstitium or the interstitial space is a contiguous fluid-filled space existing between a structural barrier, such as a cell wall or the skin, and internal structures, such as organs, including muscles and the circulatory system [14, 15, 16]. The fluid in this space is called interstitial fluid, comprises water and solutes, and drains into the lymph system [16]. The interstitial compartment is composed of connective and supporting tissues within the body – called the extracellular matrix – that are situated outside the blood and lymphatic vessels and the parenchyma of organs [16]. The interstitium/interstitial space is similar in all tissues. The structure and elements of the interstitial space are described in details in [12]. The interstitial space consists of a fibrous collagen framework that supports a gel phase containing glycosaminoglycans, salts, and plasma-derived proteins [17]. Glycosaminoglycans are polyanionic polysaccharides that are fully charged at physiologic pH. With the exception of hyaluronic acid, they are covalently bound to a protein backbone, thus creating the proteoglycans that are immobilized in the interstitium. Transport of macromolecules within the interstitium may be physically delayed by the gel structure of the proteoglycans and by electrostatic interactions with charged components of the interstitial architecture [17, 18]. A question about charge of the interstitium is open now [18, 19]. Entry of extracellular fluid and protein into the initial lymphatic vessel occurs through interendothelial openings and by vesicular transport through the endothelial cells [20]. Interendothelial openings may allow cells (macrophages, lymphocytes, erythrocytes) and cellular debris to directly enter lymphatic vessels [17]. Mechanisms of particle transport into/inside of the lymphatic vessels are reviewed in [12]. Role of a particle size and its surface properties is very important [21, 22].

Most radionuclide lymphatic flow studies use particulate materials. The agents studied include 99mTc-sulfur colloids, 99mTc-nano- and microaggregated albumin, 99mTc-antimonysulfide, 99mTc – phytate, colloidal gold particles, liposomes, and emulsions administered into the interstitial space of animals and humans [23, 24, 25 –28]. Size is the major factor determining the behavior of particulate materials after subcutaneous injection. Particles that are smaller than a few nanometers will mostly penetrate the blood capillary membrane, whereas larger particles (up to about 100 nm) can enter the lymphatic capillaries and be transported to lymph nodes. Larger particles will be trapped in the interstitial space for a long time [23]. However, the upper size limit for lymphatic uptake has not been strictly defined. Different authors have different opinions about distribution of radiotracers after an injection. Small-sized molecules (typically of size <5 nm diameter) diffuse rapidly in the interstitium and can permeate to both blood and lymphatic capillaries [29, 30]. Particles smaller than a few nanometers usually leak into blood capillaries whereas larger particles (up to about 100 nm) can enter the lymphatic capillaries and be transported to lymph nodes [23]. However, even large particles were detected in venous blood immediately after subcutaneous injection, probably as a result of direct capillary disruption by the needle [31].

The optimal colloidal size for lymphoscintigraphy is believed to be approximately 50–70 nm [27]. Individual estimates vary from 1 to 70 nm [26, 28]. Larger particles (100 nm) are believed to be trapped in the interstitial compartment for a relatively long period [23]. One study has demonstrated that transport of perfluorocarbon emulsions of $0{,}08 \div 0{,}36 \mu m$ exhibits an inverse correlation to colloid particle size [22]. The same study demonstrated that the particle surface properties may influence the uptake of colloid [22]. Lymph node uptake of colloids of similar size can vary substantially [22, 28]. Early studies with liposomes have shown that specific surface properties, such as charge, hydrophobicity, and the presence of targeting ligands, can influence both the rate of particle drainage from a subcutaneous injection site and the distribution within the lymphatic system.

The exact choice of the tracer size depends on the application [32]. For example, tracers for lymphatic flow imaging should be smaller (5–10 nm) to allow for rapid lymphatic uptake and visualization. On the other hand, the tracers for lymph node imaging should have an intermediate size (10–100 nm) in order to accumulate in the organ [34, 35, 36-39]. The optimal colloidal size for lymphoscintigraphy is believed to be approximately 50–70 nm [26]. The results of recent studies correlating the particle profile of 99mTc labeled inorganic colloids with lymph node uptake suggest that colloids with nanometric dimensions are the best suited for a high node uptake [40]. As a general rule, it can be assumed that very small nanoparticles (<10 nm) are best suited for lymphoscintigraphy, whereas large particles (>100 nm) display a longer retention in the first encountered lymph node.

The complicated anatomy of the lymphatic system, with multiple collecting vessels draining each organ and inconsistent routing of these vessels between individual subjects was a severe limitation of such studies [32]. More modern imaging approaches are based on non-invasive measures of tracer flow through draining lymph nodes or to the systemic blood circulation. Several imaging modalities have the sensitivity and resolution capable of detecting signal intensity dynamics of lymphatic tracers within lymph nodes. Such assessments have been made with positron emission tomography-computer tomography (PET/CT), magnetic resonance imaging (MRI) and fluorescence imaging techniques [41, 42, 43]. Depending on the tracer, lymph node signals will either increase steadily over time (as a measure of tracer retention) or will initially increase and then decrease (as a measure of lymph flow through the node) [3]. The first approach would be more desirable for the optimization of drug delivery or diagnostic techniques targeting the lymph node, while the second approach is more suited for assessment of lymphatic function. A group of researchers has developed a method to quantify the dynamics of NIR tracers in the draining lymph node after injection into the skin of mice [41]. Researchers have used this technique in conjunction with ICG liposomes to

demonstrate the blockage of flow through a lymph node that is bearing metastatic tumor cells and a reduction of lymphatic clearance from chronically inflamed skin [41, 44].

An alternative approach of detecting the accumulation of a lymphatic-specific tracer in the systemic blood has been developed [45, 46, 47]. As all lymphatic routes eventually lead to the bloodstream, this approach simplifies the quantification of tracer transport from a specific organ. Authors of [45] using fluorescent tracers of 40 kDa size have found that non-invasive measures of lymphatic transport to blood can be made with high sensitivity in mice by near infrared spectroscopy monitoring of the signal dynamics in a large superficial blood vessel. This method allows deeper organs or anatomical cavities to be assessed. Using these measures, researchers have demonstrated the necessity for tissue motion for tracers to access the initial lymphatic vessels of the skin. Limitations of this technique include the need for large amounts of injected tracer and the requirement of the tracer to have a long plasma circulation for sensitive dynamic assessments in the systemic blood.

2. Simulation of radiopharmaceutical transport kinetics

2.1. Mathematical simulation of radiotracer transport kinetics

Radiotracer kinetic simulation was studied by many authors [48, 49, 50]. In a typical PET study, PET data are sequentially obtained after the radioactive tracer is introduced (usually administrated intravenously) over time. The interpretation of the observed PET data over time is fulfilled in the frame of the “compartments model”, where “compartments” mean physiologically separate pools of a tracer substance. Usually authors consider four/three tissue compartments models. The first compartment is the blood. From the blood, the radiotracers move into the next compartments. The transport and binding rates of the tracers are assumed to be linearly related to the concentration differences between two compartments. Data obtained by PET detectors are obtained as the sum of these compartments. The parameters can be estimated by fitting the model to measured PET data with arterial radioactivity concentration as the input function. However this method requires the frequent manual sampling of the blood or continuous radioactivity monitoring by external radiation detectors.

Compartment model can be reversible or irreversible (containing at least one compartment which has no outlet). Application of radiotracer kinetic simulation allows us to substantiate quantitative results obtained during radionuclide diagnostic, and to connect them with morphological and functional characteristics of liver and bile-excreting systems and hemodynamic indicators [49].

Duration of a radiotracer exposure depends on the radiotracer decay rate λ. After intravenous bolus injection the radiotracer moves from one compartment to the next one. Radiotracer kinetics is described by the system of differential equations [49, 50]. The solution of such system is determination of the effective rate of accumulation/elimination. The next stage is to find all the points and use the approximation method (the smallest square, for example). Standard approach is to apply the functional of the residual function [50].

2.2. Mathematical model of radiotracer transport kinetics

Dynamic of radiotracers is a rather complicated problem. To build a correct mathematical model of radiotracer dynamics we have to take into account a very complicated anatomical structure of an organism and different physiological/ pathologic(al) processes, as well as physical and chemical processes, namely diffusion, accumulation, elimination and radioactive decay of radiotracers. The main problem is to determine the space trajectory of radiotracer movement.

After bolus intravenous administration of the radiotracers the process of transferring the radiotracers by blood vessels is begun and the so-called radiotracer “dilution” process is realized, namely the absorption of radiotracers by other organs and tissues and radiotracer decay. The injected bolus quite quickly causes a response reaction in the body.

The part of radiopharmaceuticals which is absorbed by cells is immediately metabolized, and metabolic products quickly returned to the general blood circulation. The processes taken into account in this model are the following ones:

1) radioactive decay of pharmaceuticals; 2) accumulation of pharmaceuticals in the interstitium; 3) accumulation of pharmaceuticals in the lymphatic system; 4) transport of pharmaceuticals from the blood vessels; 5) transport of pharmaceuticals and metabolites from the interstitium in the blood vessels, 6) transport of pharmaceuticals from the lymphatic system to the blood vessels.

The model of transport kinetics of radiotracers is described by a system of differential equations of the 1st order for radiotracer concentration levels in the blood-vascular system, in the interstitium, in the lymphatic system and in the urinary system. The system of equations describes the processes of accumulation/retention of radiotracers in the cells, the radiotracer elimination/washout, and radiotracer radioactive decay. This system is similar to 4-th models, where the amount of radiotracers in each compartment is proportional to the radiotracer concentration:

$$\begin{cases} \dfrac{dx}{dt} = -\lambda x(t) - \beta_{xw} x(t) + \beta_{zx} z(t) \\ \dfrac{dz}{dt} = -\lambda z(t) - (\beta_{zx} + \beta_{zu}) z(t) + \beta_{wz} w(t) \\ \dfrac{dw}{dt} = -\lambda w(t) - \beta_{wz} w(t) + \beta_{xw} x(t) \\ \dfrac{du}{dt} = -\lambda u(t) + \beta_{zu} z(t) \end{cases} . \quad (1)$$

The next denotation were used in (1): λ is the radioactive decay constant of radiotracers, $x(t)$ is the concentration of radiotracers in the interstitium, $z(t)$ is the concentration of radiotracers in blood vessels, $w(t)$ is the radiotracer concentration in the lymphatic system, $u(t)$ is the radiotracer concentration in the urinary system, β_{zx} is the rate of radiotracer capture by interstitial cells, β_{wz} is the elimination rate of radiotracers from the lymphatic system in the bloodstream, β_{xw} is the rate of radiotracer movement from the interstitium to the lymphatic system, β_{zu} is the elimination rate of radiotracers from the bloodstream. Thus, the simple system of differential equations (1) has been used to model the kinetics of radiotracers. The initial conditions are the following ones: $x(0) = 0, z(0) = 1, w(0) = 0, u(0) = 0$. Functions of activity retention $x(t), z(t), w(t), u(t)$ are presented in the reduced units (normalized on unit of the injected activity). Half-decay period of ^{99m}Tc-radiotracers is equal to $T_{1/2} = 6$ hours.

2.3. An analytical solution of the system

The solution of Cauchy problem of system (1) can be found analytically.

$$\begin{cases} x(t) = C_1 \exp(\gamma_1 t) + C_2 \exp(\gamma_2 t) + C_3 \exp(\gamma_3 t) \\ z(t) = C_1 \dfrac{\gamma_1 + A_x}{\beta_{zx}} \exp(\gamma_1 t) + C_2 \dfrac{\gamma_2 + A_x}{\beta_{zx}} \exp(\gamma_2 t) + C_3 \dfrac{\gamma_3 + A_x}{\beta_{zx}} \exp(\gamma_3 t) \\ w(t) = C_1 w_1 \exp(\gamma_1 t) + C_2 w_2 \exp(\gamma_2 t) + C_3 w_3 \exp(\gamma_3 t) \\ u(t) = C_1 u_1 (\exp(\gamma_1 t) - \exp(-\beta_{zu} t)) + C_2 u_2 (\exp(\gamma_2 t) - \exp(-\beta_{zu} t)) + C_3 u_3 (\exp(\gamma_3 t) - \exp(-\beta_{zu} t)) \end{cases} , \quad (2)$$

where coefficients $\gamma_i, i = \overline{1,3}$ are roots of the auxiliary (characteristic) equation and can be written as:

$$\gamma_1 = -\lambda - \frac{1}{3}\left(\beta_{xw} + \beta_{zx} + \beta_{wz} + \beta_{zu}\right) + \kappa_1, \gamma_2 = -\lambda - \frac{1}{3}\left(\beta_{xw} + \beta_{zx} + \beta_{wz} + \beta_{zu}\right) + \kappa_2,$$
$$\gamma_3 = -\lambda - \frac{1}{3}\left(\beta_{xw} + \beta_{zx} + \beta_{wz} + \beta_{zu}\right) + \kappa_3 \quad (3)$$

where $\kappa_i = \kappa_i(\beta_{xw}, \beta_{zx}, \beta_{wz}, \beta_{zu})$,

$$w_1 = \frac{\gamma_1^2 + \gamma_1(A_x + A_z) + A_x A_z}{\beta_{wz}\beta_{zx}}, w_2 = \frac{\gamma_2^2 + \gamma_2(A_x + A_z) + A_x A_z}{\beta_{wz}\beta_{zx}}, w_3 = \frac{\gamma_3^2 + \gamma_3(A_x + A_z) + A_x A_z}{\beta_{wz}\beta_{zx}}, \quad (4)$$

$$C_1 = \frac{\beta_{zx}(w_3 - w_2)}{-w_1\gamma_3 - w_2\gamma_1 - w_3\gamma_2 + w_2\gamma_3 + w_3\gamma_1 + w_1\gamma_2},$$
$$C_2 = \frac{\beta_{zx}(w_1 - w_3)}{-w_1\gamma_3 - w_2\gamma_1 - w_3\gamma_2 + w_2\gamma_3 + w_3\gamma_1 + w_1\gamma_2}, \quad (5)$$
$$C_3 = \frac{\beta_{zx}(w_1 - w_2)}{-w_1\gamma_3 - w_2\gamma_1 - w_3\gamma_2 + w_2\gamma_3 + w_3\gamma_1 + w_1\gamma_2}$$

$$A_x = \lambda + \beta_{xw}, A_z = \lambda + \beta_{zx} + \beta_{zu}, A_w = \lambda + \beta_{wz} \quad (6)$$

$$u_1 = \frac{\beta_{zu}(\gamma_1 + A_x)}{\beta_{zx}(w_u + \gamma_1)}, u_2 = \frac{\beta_{zu}(\gamma_2 + A_x)}{\beta_{zx}(w_u + \gamma_2)}, u_3 = \frac{\beta_{zu}(\gamma_3 + A_x)}{\beta_{zx}(w_u + \gamma_3)}. \quad (7)$$

Analytical solution (2) of the model in a form of the well-known sum-of exponential solution was obtained.

2.4. Transport parameter determination

The analytical solution of the problem contains a set of kinetic parameters or transport coefficients $\mathbf{B} = (\beta_{xw}, \beta_{uz}, \beta_{zx}, \beta_{wz})$. All parameters are positive values. The task of determination of these parameters can be solved by the residual functional $F(\beta_{xw}, \beta_{zx}, \beta_{wz}, \beta_{zu})$. For the accumulation function has been used the residual functional [49]:

$$F(\beta_{xw}, \beta_{xz}, \beta_{zx}, \beta_{wz}) = \sum_{j=1}^{N}(z_{theor}(t_j) - z_{exper}(t_j))^2 + \sum_{j=1}^{N}(x_{theor}(t_j) - x_{exper}(t_j))^2 +$$
$$+ \sum_{j=1}^{N}(w_{theor}(t_j) - w_{exper}(t_j))^2 + \sum_{j=1}^{N}(u_{theor}(t_j) - u_{exper}(t_j))^2, \quad (8)$$

where $x_{\text{exper}}(t_j)$ are measured values in the appropriate compartment. We have to determine genuine values of the problem. So we can consider the problem as a variation one. Thus it is necessary to find the minimum of the functional or find the solution of the system of equation $\begin{cases} \delta F\big|_{\mathbf{B}} = 0 \\ \delta^2 F > 0 \end{cases}$. Then the obtained values of transport coefficients $\beta_{xw}, \beta_{zx}, \beta_{wz}, \beta_{zu}$ are substituted in (2)-(7) and we have calculated the time-activity dependencies in each compartment. Moreover these dependencies are individual dosimetric characteristics. The minimization procedure is fulfilled numerically. On the basis of the time-activity dependencies one can calculate analytically the absorbed radiation dose of an injected radiotracer individual for a patient in each considered compartment.

3. Results

Radiotracer simulation is one of the main methods of interpretation of radionuclide research results. Quantitative data of radiotracer transport kinetics in the body are presented in the form of "activity-time" or "concentration-time", which reflect the spatial and temporal processes of change in the concentration of radioactive indicator in the "regions of interest" and characterize the rate of ^{99m}Tc-radiotracers retention and washout in the organ or tissue. This makes it possible to monitor changes of scintigraphy images as a function of time to assess relevant indicators of the various functions of organs and tissues which are under the treatment.

The complexity of this mathematical simulation, on one hand, is the excessive simplification of the anatomical features of the organism when it is divided into kinetic chambers, which can lead to loss or distortion of information important for diagnostics. On the other hand, excessive consideration of all possible interrelationships in the functioning of organs and systems, results in excessive number of mathematical data useless for the clinical interpretation.

The case of intravenous administration of radiotracers was considered in the model. The aim of the paper is to describe radiotracer transport in the frame of four compartment models: the circulatory system, the lymphatic system, the interstitium, and the urinary system.

The "time-activity" curves of radiotracer transport kinetic $n(t)$ in the frame of 4-compartment model can be conditionally divided into four processes $n(t) = z(t) + x(t) + w(t) + u(t)$:

- The intake of the radiotracers by the systemic blood system and the process of radiotracer distribution in the body. The vascular curve is characterized by the rapid growth of the concentration curve in the circulatory system $z(t)$ in the first seconds after injection of radiotracers, which reflects the intake of the radiotracers by the systemic blood system and beginning the process of radiotracer accumulation (curve 4 in all Figures).
- The concentration-time dependency in the interstitium $x(t)$ corresponds to the smooth amplitude growing up to the maximum value, and then entering the plateau phase, which reflects the processes of the radiotracer accumulation and retention in the interstitium (curve 2 in all Figures).
- The concentration-time dependency in the lymphatic system interstitium corresponds to the smooth amplitude growing up to the maximum value, and then entering the plateau phase, which reflects the processes of the radiotracer accumulation and retention in the lymphatic system ($x(t)$) (the plateau part of the curve 1). The concentration-time dependency in the urinary system $u(t)$ is characterizing by rapid growth and practically linear decreasing (curve 3 in all Figures), reflecting the process of radiotracer washout.

The simulation results are presented in a form of the “concentration-time” curves in each compartment (as shown in Fig. 1, 2, 3, 4). One can see that the value of the transport coefficient between to any compartment is a key parameter which influences on the concentration changes in another compartments.

3.1. The circulatory system-the interstitium transport coefficient

ISSN 2311-1100

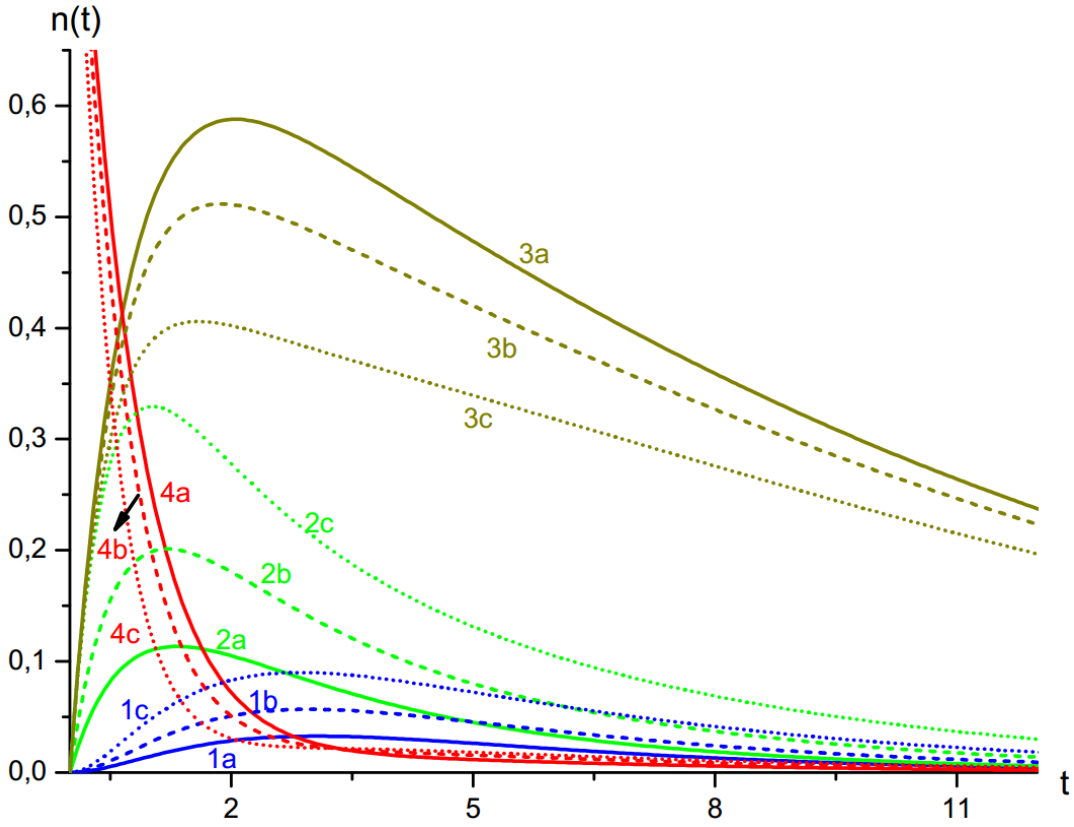

Figure 1. Concentration-time dependence, $\beta_{xw} = 0{,}25, \beta_{wz} = 0{,}5, \beta_{zu} = 1{,}00$.

1. The lymphatic system. 2. The interstitium. 3. The urinary system. 4. The circulatory system.

Different values of the transport coefficient between the circulatory system and the interstitium $a)\beta_{zx} = 0{,}25; b)\beta_{zx} = 0{,}5; c)\beta_{zx} = 1.$

ISSN 2311-1100

3.2. The interstitium-lymphatic system transport coefficient

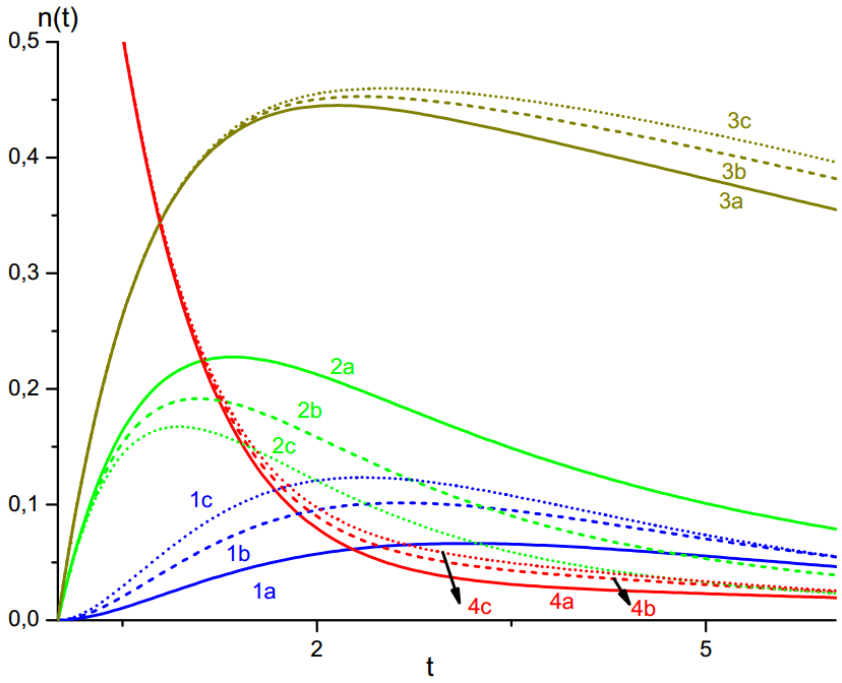

Figure 2. Concentration-time dependence, $\beta_{zx}=0{,}5;\beta_{wz}=0{,}5;\beta_{zu}=0{,}5$.

1. The lymphatic system. 2. The interstitium. 3. The urinary system. 4. The circulatory system.

Different values of the transport coefficient between the interstitium and the lymphatic system $a)\beta_{xw}=0{,}25;b)\beta_{xw}=0{,}5;c)\beta_{xw}=0{,}75$.

ISSN 2311-1100

3.3. The lymphatic system-the circulatory system transport coefficient

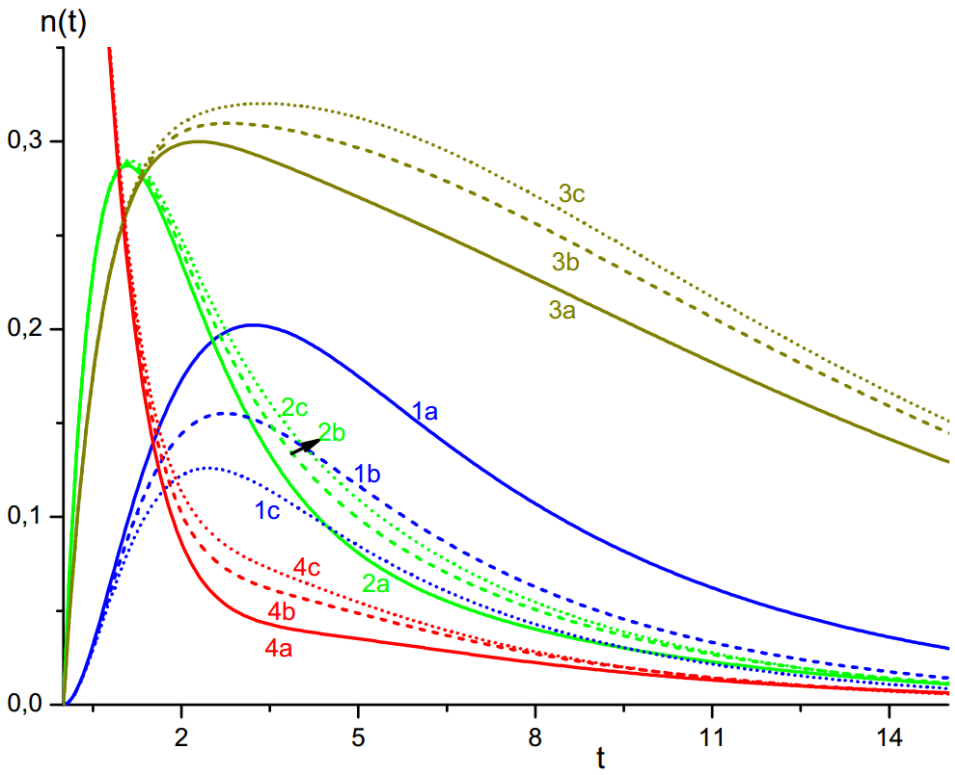

Figure 3. Concentration-time dependence, $\beta_{zx} = 0{,}75; \beta_{xw} = 0{,}5; \beta_{zu} = 0{,}5$.

1. The lymphatic system. 2. The interstitium. 3. The urinary system. 4. The circulatory system.

Different values of the transport coefficient interstitium-lymphatic system $\beta_{wz} = 0{,}25; 0{,}5; 0{,}75$.

ISSN 2311-1100

3.4. The circulatory system-the urinary system transport coefficient

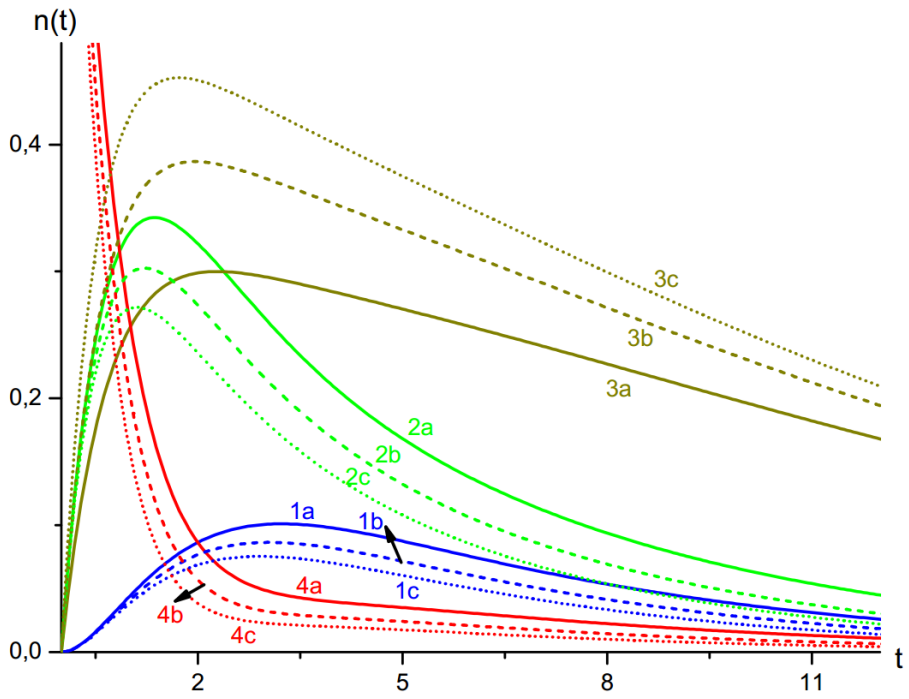

Figure 4. Concentration-time dependence, $\beta_{zx}=0{,}75;\beta_{xw}=0{,}25;\beta_{wz}=0{,}5$.

1. The lymphatic system. 2. The interstitium. 3. The urinary system. 4. The circulatory system.

Different values of the transport coefficient between the interstitium and the lymphatic system $a)\beta_{zu}=0{,}5;b)\beta_{zu}=0{,}75;c)\beta_{zu}=1{,}00$.

4. Discussions

The case of intravenous administration of radiotracers was considered in the model. The aim of the paper is to describe radiotracer transport in the frame of 4th compartment models: the circulatory system, the lymphatic system, the interstitium, and the urinary system.

The model can be easily verified by the radioactive tracer concentration data in the circulatory/lymphatic system measured at some time points, and the obtained data can be used to determine of the transport coefficients. Time-activity dependencies were obtained and analyzed for each compartment. The model can be used for individual transport parameter calculation at administration by therapeutic dose loads.

The proposed model can be classified as a simple model taking into account the main circulation process of radiotracers in a body. It can by improved by introduction of the additional compartments. The model can be transformed for different ways of radiotracer administration.

In this model it is easy to estimate the transport coefficients for individual patients and forecast absorbed radiation doses in each chamber.

5. Conclusions

The proposed four-compartment mathematical model describes transport kinetics of 99m-technetium radiotracers at intravenous administration process with taking into account radiopharmaceutical accumulation, elimination and radioactive decay. Analytical solution of the model in a form of the well-known sum-of exponential solution was obtained. The dependencies of the tracer concentration versus the time are analyzed. The model can be easily verified by the radioactive tracer concentration data in the circulatory/lymphatic system measured at some time points, and the obtained data can be used to determine of the transport coefficients. Time-activity dependencies were obtained and analyzed for each compartment. The model can be used for individual transport parameter calculation at administration by therapeutic dose loads.

Integration of the mathematical model with experimental or clinical data can provide a better tool to understand the radiopharmaceuticals distribution, accumulation and elimination processes, in particular, to evaluate time of accumulation and retention of ^{99m}Tc radiotracers in the “region of interest”. The use of radiotracer transport kinetic model will make it possible to connect some physical indicators with definite physiological processes to evaluate the investigation results, and present the objective evaluation of functional state of the investigated organ according to the obtained radiological data.

Disclaimers: The author declares that they have no financial or personal relationships that may have inappropriately influenced them in writing this article.

Conflict of interest statement: The authors state that there are no conflicts of interest regarding the publication of this article.

ISSN 2311-1100
ORCID

Oksana SHEVTSOVA: **https://orcid.org/0000-0002-6316-135X**

REFERENCES:

1. I. Khakhaly, J. Maublant, S.Goldsmith, *Nuclear Oncology: diagnostic and therapy*. Eds., Philadelphia: Lippincott Williams&Wilkins, 2001, 563.

2. L. Manni, Rambaldi P., E. Procaccini, et al., Scintimammography with Technetium-99m Tetraphosmin in the diagnosis of breast cancer and lymph node metastases. Eur. J. Nucl. Med., 1996; 23(8): 932-939.

3. B.E. Hillner, Decision Analysis: MIBI Imaging of Nonpalpable Breast Abnormalities, J. Nucl. Med, 1997; 38: 1772-1778, PMID: 9374352

4. A.M. Al-Shammari, A.H. Elgazzar, A. Ashkanami Rasha, ^{99Tc}MIBI Whole Body Scan: A Potentially Useful Technique for Evaluating Metabolic Bone Disease, World J. Nucl. Med., 2013; 12(1): 8-13, doi: 10.4103/1450-1147.113934

5. J.A. Ponto, Mechanisms of Radiopharmaceutical Localization, UNM College of Pharmacy, 16(4), 2012.

6. V.Yu. Kundin, Characteristic of main radiopharmaceuticals for kidney investigation: modern state and further perspectives, Ukrainian Radiological Journal, XII (1), 2004; 79-87.

7. K. Schwochau, Technetium. Wiley-VCH, 2000.

8. Yu. B. Lishmanov and V.I. Chernov, Radionuclide diagnostic. Eds., Tomsk: STT, 2004: 394.

9. M. Piga, P. Bolasco, L. Satta L., Double-phase parathyroid technetium-99m-MIBI scintigraphy to identify functional autonomy in secondary hyperparathyroidism. J. Nucl. Med., 1996; 37: 565-569, PMID: 8691240.

10. I. Ak, JAK Blokland, EKJ Pauwels, et al., The clinical value of 18F-FDG detection with a dual-head coincidence camera: a review. Eur J Nucl Med, 2001; 28: 763–778, doi: 10.1016/S0720-048X(02)00003-7.

11. Miwa Sato, Naoki Sasaki, Manabu Ato, Satoshi Hirakawa, Kiichi Sato, Kae Sato, Microcirculation-on-a-Chip: A Microfluidic Platform for Assaying Blood- and Lymphatic Vessel Permeability, PLOS ONE, 2001; 10(9): 1/18-18/18, doi:10.1371/journal.pone.0137301.

12. Andrzej Szuba, William S. Shin; H. William Strauss, and Stanley Rockson, The Third Circulation: Radionuclide Lymphoscintigraphy in the Evaluation of Lymphedema, Journal of Nuclear Medicine, 2003; 44(1): 43-57, PMID: 12515876

13. D.C. Zawieja, Contractile physiology of lymphatics, Lymphat. Res. Biol., 2009; 7: 87–96, doi: 10.1089/lrb.2009.0007

14.https://en.wikipedia.org/wiki/Interstitium

15. J.L. Bert, R.H. Pearce, *The interstitium and microvascular exchange. In: Handbook of Physiology. The Cardiovascular System. Microcirculation* (sect. 2; pt. 1; chapt. 12; vol. IV ed.). Bethesda, MD: American Physiological Society. 1984: 521–547. ISBN 0683072021.

16. H. Wiig, M.A. Swartz, Interstitial fluid and lymph formation and transport: Physiological regulation and roles in inflammation and cancer. Physiological Reviews, 2012; 92(3):1005–1060. doi: 10.1152/physrev.00037.2011.

17. F. Ikomi, G. Schmid-Schonbein, Lymph transport in the skin. Clin Dermatol, 1995; 13: 419–427, doi: 10.1016/0738-081x(95)00089-x

18. T.J. Ryan, D. De Berker, The interstitium, the connective tissue environment of the lymphatic, and angiogenesis in human skin. Clin Dermatol., 1995; 13: 451–458.

19. K. Aukland, R.K. Reed, Interstitial-lymphatic mechanisms in the control of extracellular fluid volume. Physiol Rev, 1993; 73: 1–78, doi: 10.1016/0738-081x(95)00091-s

20. F. Ikomi, G. K. Hanna, G.W. Schmid-Schonbein, Mechanism of colloidal particle uptake into the lymphatic system: basic study with percutaneous lymphography. Radiology, 1993; 196: 107–113, doi: 10.1148/radiology.196.1.7784553

21. F. Ikomi, J. Hunt, G. Hanna, G. W. Schmid-Schonbein, Interstitial fluid, plasma protein, colloid, and leukocyte uptake into initial lymphatics. J Appl Physiol, 1996; 81: 2060–2067, doi: 10.1152/jappl.1996.81.5.2060

22. F. Ikomi, GK Hanna, G. W. Schmid-Schonbein, Size- and surface-dependent uptake of colloid particles into the lymphatic system. Lymphology, 1999; 32: 90–102, PMID: 10494521

23. S.M. Moghimi, B. Bonnemain, Subcutaneous and intravenous delivery of diagnostic agents to the lymphatic system: applications in lymphoscintigraphy and indirect lymphography, Adv. Drug Deliv. Rev., 1999; 37: 295–312 , doi: 10.1016/s0169-409x(98)00099-4

24. G.N. Ege Radiocolloid lymphoscintigraphy in neoplastic disease. Cancer Res., 1980; 40: 3065–3071, PMID: 7397701

25. Ching-Chun Ho, Yu-Hung Chen, Shu-Hsin Liuc, Hwa-Tsung Chen, Ming-Che Lee, Optimal imaging time for Tc-99m phytate lymphoscintigraphy for sentinel lymph node mapping in patients with breast cancer, Tzu Chi Medical Journal, 2019; 31(3): 163–168, doi: 10.4103/tcmj.tcmj_88_18

26. L. Bergqvist, S.E. Strand, B.R. Persson. Particle sizing and biokinetics of interstitial lymphoscintigraphic agents, Semin. Nucl. Med., 1983; 13: 9–19, doi: 10.1016/s0001-2998(83)80031-2

27. S.E. Strand, L. Bergqvist, Radiolabeled colloids and macromolecules in the lymphatic system, Crit Rev Ther Drug Carrier Syst., 1989; 6: 211–238, PMID: 2692844

28. S.E. Strand, B.R. Persson, Quantitative lymphoscintigraphy I: basic concepts for optimal uptake of radiocolloids in the parasternal lymph nodes of rabbits, J. Nucl. Med., 1979; 20: 1038–1046, PMID: 231640

29. Y. Niki, M. Ogawa, R. Makiura, Y. Magata, C. Kojima, Optimization of dendrimer structure for sentinel lymph node imaging: effects of generation and terminal group, Nanomed-Nanotechnol., 2015; 11: 2119–2127.

30. S.T. Proulx, P. Luciani, A. Christiansen, S. Karaman, K.S. Blum, M. Rinderknecht, J.C. Leroux, M. Detmar, Use of a PEG-conjugated bright near-infrared dye for functional imaging of rerouting of tumor lymphatic drainage after sentinel lymph node metastasis, Biomaterials, 2013; 34: 5128–5137, doi: 10.1016/j.biomaterials.2013.03.034

31. A.A. Fokin, F. Robicsek, T.N. Masters, G.W. Schmid-Schonbein, S. H.Jenkins, Propagation of viral-size particles in lymph and blood after subcutaneous inoculation, Microcirculation, 2000; 7: 193–200, PMID: 10901498

32. A.K. Polomska, S.T. Proulx, Advanced Drug Delivery Reviews, 2021; 170: 294–311.

33. S. Modi, A.W. Stanton, P.S. Mortimer, J.R. Levick, Clinical assessment of human lymph flow using removal rate constants of interstitial macromolecules: a critical review of lymphoscintigraphy, Lymphat. Res. Biol., 2007; 5: 183–202, doi: 10.1089/lrb.2007.5306

34. S.T. Proulx, P. Luciani, L.C. Dieterich, S. Karaman, J.C. Leroux, M. Detmar, Expansion of the lymphatic vasculature in cancer and inflammation: new opportunities for in vivo imaging and drug delivery, J. Control. Release, 2013; 172: 550–557. doi: 10.1016/j.jconrel.2013.04.027

35. J. Li, Z. Zhuang, B. Jiang, P. Zhao, C. Lin, Advances and perspectives in nanoprobes for noninvasive lymph node mapping, *Nanomedicine (London)*, 2015; 10: 1019–1036. doi: 10.2217/nnm.14.201

36. N.L. Trevaskis, L.M. Kaminskas, C.J. Porter, From sewer to saviour - targeting the lymphatic system to promote drug exposure and activity, Nat. Rev. Drug Discov., 2015; 14: 781–803. doi: 10.1038/nrd4608

37. A. Schudel, D.M. Francis, S.N. Thomas, Material design for lymph node drug delivery, Nat. Rev. Mater., 2019; 4: 415–428. doi: 10.1038/s41578-019-0110-7

38. Z. Yang, R. Tian, J.J. Wu, Q.L. Fan, B.C. Yung, G. Niu, O. Jacobson, Z.T. Wang, G. Liu, G.C. Yu, W. Huang, J.B. Song, X.Y. Chen, Impact of semiconducting perylene diimide nanoparticle size on lymph node mapping and cancer imaging, ACS Nano, 2017; 11: 4247–4255. doi: 10.1021/acsnano.7b01261

39. X. Yang, Z. Wang, F. Zhang, G. Zhu, J. Song, G.J. Teng, G. Niu, X. Chen, Mapping sentinel lymph node metastasis by dual-probe optical imaging, Theranostics, 2017; 7: 153–163. doi: 10.7150/thno.17085

40. E.G., Nunez, et al., Influence of colloid particle profile on sentinel lymph node uptake, Nucl. Med. Biol., 2009; 36: 741–747. doi: 10.1016/j.nucmedbio.2009.04.009

41. S.T. Proulx, P. Luciani, S. Derzsi, M. Rinderknecht, V. Mumprecht, J.C. Leroux, M. Detmar, Quantitative imaging of lymphatic function with liposomal indocyanine green, Cancer Res., 2010; 70: 7053–7062. doi: 10.1158/0008-5472.CAN-10-0271

42. Q. Ma, Y. Decker, A. Müller, B.V. Ineichen, S.T. Proulx, Clearance of cerebrospinal fluid from the sacral spine through lymphatic vessels, J. Exp. Med., 2019; 216: 2492–2502. doi: 10.1084/jem.20190351

43. D.L.J. Thorek, D.S. Abou, B.J. Beattie, R.M. Bartlett, R.M. Huang, P.B. Zanzonico, J. Grimm, Positron lymphography: multimodal, high-resolution, dynamic mapping and resection of lymph nodes after intradermal injection of F-18-FDG, J. Nucl. Med., 2012; 53(9): 1438–1445. doi: 10.2967/jnumed.112.104349

44. R. Huggenberger, S. Ullmann, S.T. Proulx, B. Pytowski, K. Alitalo, M. Detmar, Stimulation of lymphangiogenesis via VEGFR-3 inhibits chronic skin inflammation, J. Exp. Med., 2010; 207 (10): 2255–2269. doi: 10.1084/jem.20100559

45. S.T. Proulx, Q. Ma, D. Andina, J.C. Leroux, M. Detmar, Quantitative measurement of lymphatic function in mice by noninvasive near-infrared imaging of a peripheral vein, JCI Insight, 2017; 2(1): 1-12. doi: 10.1172/jci.insight.90861

46. D. Tobbia, J. Semple, A. Baker, D. Dumont, A. Semple, M. Johnston, Lymphedema development and lymphatic function following lymph node excision in sheep, J. Vasc. Res., 2009; 46(5): 426–434. https://doi.org/10.1159/000194273

47. A. Baker, J.L. Semple, S. Moore, M. Johnston, Lymphatic function is impaired following irradiation of a single lymph node, Lymphat. Res. Biol., 2014; 12: 76–88. doi: 10.1089/lrb.2013.0036

48. Hiroshi Watabe, Yoko Ikoma, Yuichi Kimura, Mika Naganawa, and Miho Shidahara, PET kinetic analysis—compartmental model, Annals of Nuclear Medicine, 2006; 20(9): 583–588. doi: 10.1007/BF02984655

49. A.V. Matveev, M.Yu. Korneeva, Peculiarities of radiotracer kinetic simulation at functional investigation of the hepatobiliary system, *Vestnik of Omsk University*, 1995; #3: 42-51 (in Russian).

50. A.S. Lunev, Mathematical Simulation of Transport Kinetics of radiopharmaceutical 68-Ga-citrate for PET imaging of inflammation. Meditsinskaya Radiologia I Yadernaya Bezopasnost (in Russian) (Medical Radiology and radiation safety), 2015; 60(6): 42-47.

ISSN 2311-1100

PLAGIARISM REPORT:

АНТИПЛАГИАТ
ОБНАРУЖЕНИЕ ЗАИМСТВОВАНИЙ

Отчет о проверке на заимствования №1

Автор: 4141184@kntu.net.ua / ID: 9432678
Проверяющий: (4141184@kntu.net.ua / ID: 9432678)

Отчет предоставлен сервисом «Антиплагиат»

ИНФОРМАЦИЯ О ДОКУМЕНТЕ

№ документа: 1
Начало загрузки: 10.11.2021 08:25:51
Длительность загрузки: 00:00:00
Имя исходного файла: O_Shevtsova_A Mathematical model.pdf
Название документа: O_Shevtsova_A Mathematical model
Размер текста: 30 кБ
Символов в тексте: 30772
Слов в тексте: 4464
Число предложений: 275

ИНФОРМАЦИЯ ОБ ОТЧЕТЕ

Начало проверки: 10.11.2021 08:25:52
Длительность проверки: 00:00:02
Комментарии: не указано
Модули поиска: Интернет

ЗАИМСТВОВАНИЯ *	САМОЦИТИРОВАНИЯ	ЦИТИРОВАНИЯ	ОРИГИНАЛЬНОСТЬ
33,28%	0%	0%	66,72%

Заимствования — доля всех найденных текстовых пересечений, за исключением тех, которые система отнесла к цитированиям, по отношению к общему объему документа.
Самоцитирования — доля фрагментов текста проверяемого документа, совпадающий или почти совпадающий с фрагментом текста источника, автором или соавтором которого является автор проверяемого документа, по отношению к общему объему документа.
Цитирования — доля текстовых пересечений, которые не являются авторскими, но система посчитала их использование корректным, по отношению к общему объему документа. Сюда относятся оформленные по ГОСТу цитаты; общеупотребительные выражения; фрагменты текста, найденные в источниках из коллекций нормативно-правовой документации.
Текстовое пересечение — фрагмент текста проверяемого документа, совпадающий или почти совпадающий с фрагментом текста источника.
Источник — документ, проиндексированный в системе и содержащийся в модуле поиска, по которому проводится проверка.
Оригинальность — доля фрагментов текста проверяемого документа, не обнаруженных ни в одном источнике, по которым шла проверка, по отношению к общему объему документа.
Заимствования, самоцитирования, цитирования и оригинальность являются отдельными показателями и в сумме дают 100%, что соответствует всему тексту проверяемого документа.
Обращаем Ваше внимание, что система находит текстовые пересечения проверяемого документа с проиндексированными в системе текстовыми источниками. При этом система является вспомогательным инструментом, определение корректности и правомерности заимствований или цитирований, а также авторства текстовых фрагментов проверяемого документа остается в компетенции проверяющего.

№	Доля в отчете	Источник	Актуален на	Модуль поиска
[01]	28,16%	Mathematical Simulation of Transport Kinetics of Tumor-Imaging Radiopharmaceutical 99mTc-MIBI https://hindawi.com *Це публікація автора.	02 Сен 2017	Интернет
[02]	0%	Mathematical Simulation of Transport Kinetics of Tumor-Imaging Radiopharmaceutical 99mTc-MIBI https://hindawi.com	09 Янв 2021	Интернет
[03]	3,17%	Lymphedema || https://doi.org	11 Сен 2019	Интернет